

## Polaritonic and Photonic Gap Interactions in a Two-Dimensional Photonic Crystal

Andreas Rung and Carl G. Ribbing

*Division of Solid State Physics, Department of Engineering Science, Uppsala University, Uppsala, Sweden*  
*Department of Functional Materials, Division of Sensor Technology, Swedish Defence Research Agency, Linköping, Sweden*  
 (Received 30 June 2003; published 25 March 2004)

If an ionic material is used in a photonic crystal, the lattice resonance creates a polaritonic gap in the infrared range. The interaction between a polaritonic gap and the structure gap in a 2D square photonic crystal is studied by transfer matrix photonic band structure calculations. The polaritonic gap appears for a surprisingly low volume density of the ionic material. The TM gaps are larger than the TE gaps, as in the dielectric case. By varying the lattice constant, the structure gaps can be shifted across the polaritonic gap, and the effects of merging the two gaps can be studied.

DOI: 10.1103/PhysRevLett.92.123901

PACS numbers: 42.70.Qs, 41.20.Jb, 42.25.Bs, 71.36.+c

During the past 15 years, a new subfield in photonics or optics has been created with the advent of photonic crystals, i.e., periodic structures with unit cell dimensions that correspond to the wavelength of ordinary light. Early work focused on the possibility to quench optical deexcitation by placing an excited atom within a matrix lacking the final states of the deexcitation process [1,2]. The continued development benefited from the close analogies with the established theory for the electronic structure of ordinary (atomic) crystals. The light line, i.e., the dispersion of light in a homogenous solid, develops into a structure of branches that vary with the direction of the wave vector in the unit cell. The concepts of solid state theory such as Brillouin zone, band structure, and, in particular, energy gaps were readily transferred into this new area [3]. In particular, the experimental verification of *photonic gaps*, i.e., frequency or energy intervals within which electromagnetic waves cannot propagate in the periodic structure, created a vivid interest. It is debatable to what extent the photonic gaps were a fundamentally novel physical phenomena [4], but the interest was spurred by the close analogies with electronic structure and the prospects of optoelectronic applications. In the gap region, a photonic crystal exhibits total reflectance and zero emittance which suggests many applications. Even more possibilities appeared when it was realized that the defect state in a large enough photonic gap [5] represents an almost lossless communication channel. The preparation of photonic crystals, designed with successively smaller lattice constants, became a challenge that has been successfully met, down to near infrared and even visible wavelengths [6].

Originally, the materials used both in theoretical and experimental work were nonabsorbing with negligible dispersion. The impetus of the work was the possibility to make a periodic structure of a high index dielectric and air totally reflecting. This would be the two- or three-dimensional analogue of a dielectric multilayer mirror [7]. This required *complete* photonic gaps, i.e., total reflectance for both polarizations at all angles of incidence.

At a later stage, the field evolved to study the influence of absorption and dispersion in one of the material components in a photonic crystal. Dispersion introduces a difficulty with calculational schemes within which the photon energy/frequency is calculated for a fix wave vector  $\mathbf{K}$ , which is typical for the plane wave (PW) method [3]. Sigalas *et al.* [8] handled this by using a multistep, piecewise constant dielectric function. Alternatively, one can use the transfer matrix method (TMM) in which the reverse calculation  $\mathbf{K} = \mathbf{K}(\omega)$  is made, permitting the use of a periodic and dispersive dielectric function

$$\varepsilon(\mathbf{R} + \mathbf{r}, \omega) = \varepsilon(\mathbf{r}, \omega), \quad (1)$$

where  $\mathbf{R}$  is a lattice translation in the photonic crystal. By definition, a band structure is valid for a periodic and infinite structure. However, the TMM also permits calculations of transmittance through, and reflectance from, photonic crystals with an arbitrary finite thickness.

Studies of photonic crystals with metal components have given very interesting results. The dielectric function of bulk metals below the plasma frequency is negative, which shows up as a wide gap in the band structure [9,10]. It was also demonstrated that the configuration of the metal had a large influence on the behavior. Using very fine wires, 1  $\mu\text{m}$ , in a periodic structure, Pendry [11] showed that the combined result of low effective electron density, and induction from the magnetic field around the wires, reduced the plasma frequency with 6 orders of magnitude. The remarkable effect is that a very low metallic density periodic grid—visibly transparent—would be reflective for, e.g., microwaves. Using a multiple scattering method and including also the absorption of metals, it was shown that, in spite of the presence of metallic absorption, the scaling of gap positions holds approximately. In contrast to Pendry, Sievenpiper *et al.* [12] used strong *capacitive* coupling between metal islands separated by polyimide, i.e., metal patches on a circuit board. Also in this case, a wide gap at low frequencies is noted. The top of the “valence band” is depressed by the capacitive coupling, while the position of the “conduction

band” is controlled by the lattice constant of the metallo-dielectric lattice.

In this Letter, we report on TMM calculations for a 2D photonic crystal made up from air and an ionic material in the Reststrahlen band frequency region, i.e., the thermal infrared. In a Reststrahlen region, the dielectric function is both negative and strongly dispersive, i.e., similar to a metal, due to a TO lattice resonance. However, the material is optically metal-like only over a limited frequency interval,  $\omega_T < \omega < \omega_L$ , where  $\omega_T$  and  $\omega_L$  are the  $q = 0$  phonon frequencies for the TO- and LO-phonon branches, respectively. The ionic crystals are dielectric in the visible range. Furthermore, the material is nonconducting, electronic induction and screening currents do not complicate the situation. Our study continues some of the studies made in Ref. [8] by Sigalas *et al.* and it is complementary to very recent work by Huang *et al.* [13]. We shall adopt their terminology, i.e., refer to the gap in the photonic band structure that is directly linked to the photon-phonon interaction in one material as *polaritonic*, and the crystal as such a “polaritonic photonic crystal” (PPC [13]). When necessary to distinguish, we denote the gaps based on the crystalline long range order as *structure* gaps. In [13], the electro-optical materials CsI and LaTiO<sub>3</sub> are used as examples of ionic materials, while we shall use ceramic BeO to illustrate the effect. 2D photonic crystals with an ionic component have also been studied with multiple scattering calculations [14,15].

Our calculations have been made with a transfer matrix program package OPAL [16], which in cases with dispersion has an intrinsic advantage in comparison with PW methods. The case of dielectric 2D photonic crystals, including out-of-plane band structure, has been thoroughly analyzed by the MIT group [17]. They studied both square and triangular lattices, with circular cylinders of air or a dielectric ( $\epsilon = 11.43$ ) as a function of  $r/a$ , i.e., the linear density of cylinders. They demonstrate that square lattices, even with this high contrast, have *no* complete photonic gap (in contrast to triangular lattices). This is primarily caused by the almost absence of TE gaps, while some TM bands are separated by gaps for a range of  $r/a$  values.

The input values for our calculations, the dielectric function for beryllium oxide, were obtained from published data [18,19]. A single oscillator model was used:

$$\epsilon = \epsilon_\infty + \frac{[\epsilon(0) - \epsilon_\infty]\omega_T^2}{(\omega_T^2 - \omega^2 - i\omega\gamma)}. \quad (2)$$

For the ceramic case, we used an average  $h\nu_T = 87.0$  meV, damping  $h\gamma = 11.51$  meV, and obtained  $h\nu_L$  from  $\epsilon_0$ ,  $\epsilon_\infty = 2.99$ , and the Lyddane-Sachs-Teller relation. In Fig. 1, we reproduce the real,  $\epsilon_1(h\nu)$ , and imaginary,  $\epsilon_2(h\nu)$ , parts of the model BeO dielectric function, as functions of photon energy,  $h\nu$ , with some of the parameter values indicated. In particular around the resonance, the dispersion is very strong, shifting the  $\epsilon_1$  values

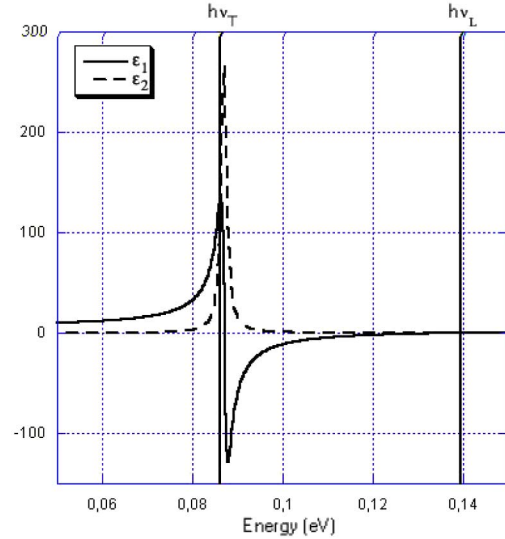


FIG. 1 (color online). The real and imaginary parts of the model complex dielectric function for beryllium oxide. The oscillator model energy parameter values of the TO resonance  $h\nu_T$  and the LO resonance  $h\nu_L$  are indicated.

from high positive to negative values in an energy interval width of the order  $h\gamma$ . It was shown that this strong dispersion around  $\omega_T$  causes flux expulsion and node switching, i.e., strong shifts of the mode pattern in the crystal over a narrow frequency range [13].

In Fig. 2, we show the calculated band structures. The flat bands of localized modes immediately below  $\omega_T$  as shown in [13–15] are suppressed in our calculations. The  $K$  axis has the usual symmetry point notation for a 2D Brillouin zone. There are, however, two unconventional features. The TO phonon resonance introduces a definite energy into the calculation. Our results are thus not generic, as in the standard case. We have therefore preferred to use photon energy in eV, not the usual dimensionless units, on the y axis. More importantly, we have also included part of the results obtained in the gap regions, i.e., imaginary wave-vector solutions,  $\text{Im}[K]$ . The magnitude of this variable gives information about the damping in the structure, the inverse of which could be named a “photonic skin depth.”

Considering first the real part, one notices the large polaritonic gap around 0.1 eV. Not surprisingly, but in contrast to a dielectric photonic crystal, it is a complete gap. The stop band effect of a Reststrahlen band is strong enough, even in the unfavorable case of a square structure. It is not tied to symmetry effects, so it is not positioned at a zone boundary. The magnitudes of the resulting TM and TE gap nevertheless shift with direction in the structure. The gap in the  $M$ - $\Gamma$  direction is 30% larger than that in the  $\Gamma$ - $X$  direction, as seen from the band edges in this diagram. The packing density  $r/a = 0.16$  is low, i.e., far from close packed, which occurs for  $r/a = 0.5$ . Just like the structure gaps in Ref. [17], the polaritonic gap in Fig. 2 is smaller for TE than for TM

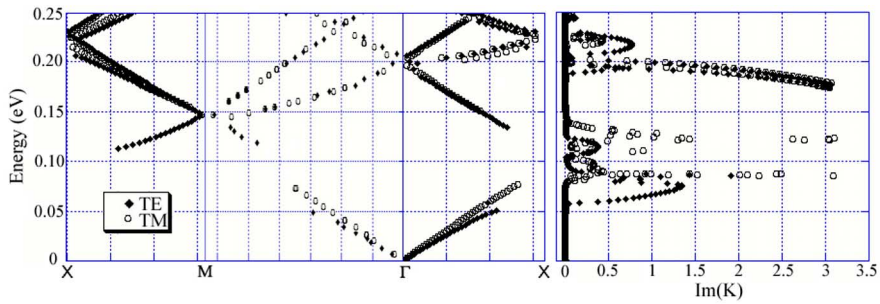


FIG. 2 (color online). Photonic band structure for a square lattice of BeO rods in air with lattice constant  $a = 6.0 \mu\text{m}$  and  $r/a = 0.16$ . The three sections to the left give the normal, real band structure, and the rightmost part is plotted vs  $\text{Im}[\mathbf{K}]$ .

modes, mainly because the TE "valence band" is shifted upwards compared to the lower edge of the TM modes. Intuitively it is understandable that a horizontal electric field scatters more weakly off the vertical cylinders than a vertical field. Beside the appearance of the polaritonic gap around 0.1 eV, the dispersion in the BeO model, as shown in Fig. 1, has a strong influence upon the entire band structure, which has fewer bands with strong dispersion in a given energy interval than would a nondispersive, purely dielectric crystal have.

We now turn our attention to the  $\text{Im}[\mathbf{K}]$  part of Fig. 2. These evanescent states do not extend through the crystal, so they do not obey the Bloch theorem, and are not limited to a Brillouin zone. Our calculations gave two types of gap solutions in  $h\nu$  vs  $\text{Im}[\mathbf{K}]$ : loops with moderate  $K$  values that are closed across the gaps, and parabolic shaped curves extending asymptotically to large  $K$  values. It is interesting that the same two types of solutions were recently observed for the case of electronic tunneling through a ferromagnet/insulator/ferromagnet junction [20].

In Fig. 3 we show, to the left, the  $\Gamma$ -X part of a band structure for a somewhat higher packing density,  $r/a = 0.25$ . To the right, the transmittance spectrum for a 2D crystal with the thickness  $16a$  is reproduced. We notice a

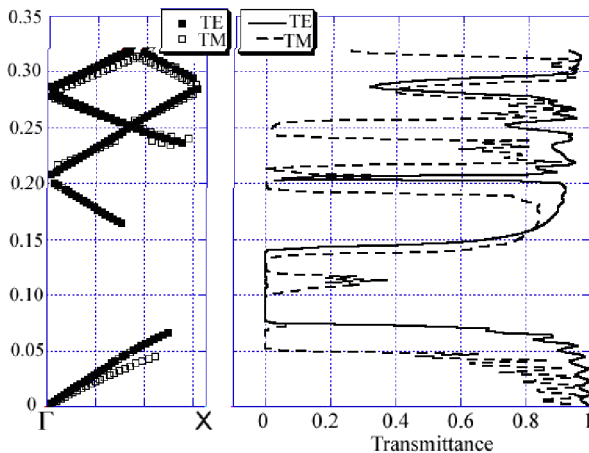


FIG. 3 (color online). The  $\Gamma$ -X part of the photonic band structure for a square lattice of BeO rods in air with  $a = 5.6 \mu\text{m}$  and  $r/a = 0.25$ . The right panel is the infrared transmittance spectrum for normal incidence in the  $\Gamma$ -X direction towards a 16 lattice constants thick crystal.

slight increase of the gap width compared with Fig. 2, which is natural considering the density of the Reststrahlen material is higher. However, part of this increase is due to overlap with a structural TE gap. We shall illustrate these effects more systematically below. The right-hand panel confirms the efficiency of the stop band. In this particular case, it is the TE modes that are effectively blocked over a connected gap with  $\Delta\nu/\nu_0 \approx 0.5$ , which is a high value compared with what is encountered in dielectric cases [3]. The TM modes instead have two disconnected gaps. This can be understood as the effect of the upward shift of the TE modes noted above.

Next we shall show more complete results for the variation of photonic gaps as a function of linear packing density,  $r/a$ . In this Letter, we do not have the ambition to give a complete "gap map" as reported previously for dielectric 2D crystals [17]. We have chosen a phenomenologically defined "gap" as the energy intervals, within which the transmittance for normal incidence in the  $\Gamma$ -X direction upon a 16 layer photonic crystal is  $< 0.2$ . In Fig. 4, we have collected such gap widths for the lattice constant  $a = 2.8 \mu\text{m}$ , as a function of  $r/a$ . The closed and the open symbols distinguish between upper and lower gap edges, respectively. We can observe the different behavior of the polaritonic and structure gaps. The polaritonic gap is centered on the  $h\nu_T - h\nu_L$  interval as seen in Fig. 1, and grows with increasing  $r/a$ , i.e., volume fraction of BeO. For low  $r/a$  values, this gap exists for lower values than one might have expected, even if there

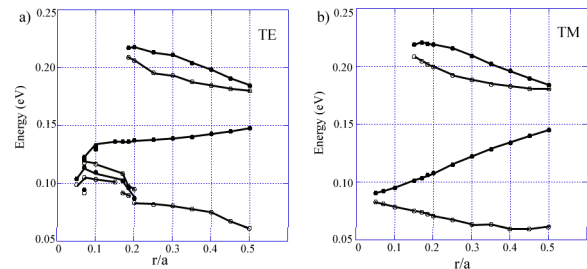


FIG. 4 (color online). The variation of the polaritonic and structure gap edges with linear packing density  $r/a$  for the lattice constant  $a = 2.8 \mu\text{m}$ . The gaps have been defined as described in the text by the  $\Gamma$ -X normal incidence transmittance of a 16 layer photonic crystal  $< 0.2$  for (a) TE modes and (b) TM modes. The closed and the open symbols distinguish between upper and lower gap edges, respectively.

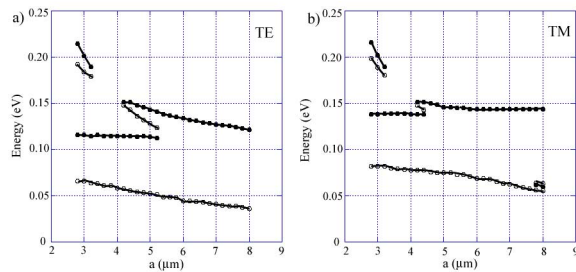


FIG. 5 (color online). The variation of the polaritonic and structure gap edges with linear packing density  $r/a = 0.25$  as functions of the lattice constant  $a$ . The gaps have been defined as in Fig. 4. The closed and open symbols distinguish between upper and lower gap edges, respectively. The two diagrams refer to (a) TE modes and (b) TM modes.

were some problems to resolve the edges. It is significant down to  $r/a \approx 0.05$ , i.e., a volume density  $< 1\%$ . As with the dimensionless frequency:  $(\omega a)/(2\pi c)$ ; in the nondispersive case in Ref. [17], the frequency positions of structure gaps decrease, with increasing  $r/a$  values. We also observe the existence of an  $r/a$  value that maximizes the width of a structure gap, at a density that is well below that of close packed. This is in agreement with the behavior of 3D dielectric photonic crystals, e.g., the OPAL structure should be less than close packed in order to maximize the structure gap [5].

In Fig. 5, we show the gap width variations as a function of lattice constant  $a$ , for a fixed packing fraction  $r/a = 0.25$ . We notice that the TE structure and polariton gaps merge for  $a \approx 5.3 \mu\text{m}$ , while the TM gaps are separate until  $a \approx 4.4 \mu\text{m}$ . It is striking to see that, even before this merging, the lower edge of what was the polariton gap shifts downwards with increasing  $a$  values. This is a manifestation of structure and polaritonic gap interaction that we believe deserves more detailed investigation. Such a study may result in a new tool for photonic band gap engineering [21]. In this case, the density of the absorbing material is constant, because  $r/a$  is constant, but the ratio between the rod radii and the resonance wavelength is increasing. As noted in Ref. [13], there are good reasons to believe that polaritonic gaps will appear also in 3D crystals. 3D calculations, however, in cases with strong dispersion will be quite extensive and possibly suffer from numerical instabilities.

In summary, we have performed model photonic band structure calculations for a square 2D photonic crystal of rods with a Reststrahlen band. This entails strong material dispersion and absorption in one component. The results verify the representation of the frequency range with a negative dielectric function, as an interval with only imaginary wave-vector solutions and a large polaritonic band gap. By varying the packing density or the lattice constant, we have demonstrated the interaction

between this polaritonic gap, tied to one of the materials, and a regular photonic gap that is based on optical contrast and long range symmetry of the photonic crystal.

We are grateful to Professor John Pendry and Dr. Andrew Ward of Imperial College London for giving us OPAL and instructions on how to use it. We have benefited from several discussions with Dr. Jan Fagerström, FOI, Linköping, regarding the effects of dispersion on photonic band structures. Our work has been sponsored by The Swedish Research Council and the Swedish Defence Research Agency.

- 
- [1] E. Yablonovitch, Phys. Rev. Lett. **58**, 2059 (1987).
  - [2] S. John, Phys. Rev. Lett. **53**, 2169 (1984).
  - [3] J. D. Joannopoulos, R. D. Meade, and J. N. Winn, *Photonic Crystals* (Princeton University Press, Princeton, NJ, 1995).
  - [4] C. G. Ribbing, in *Optical Interference Coatings*, Springer Series in Optical Sciences Vol. 88, edited by N. Kaiser and H. K. Pulker (Springer-Verlag, Heidelberg, 2003), p. 35.
  - [5] E. Yablonovitch, J. Mod. Opt. **41**, 173 (1994).
  - [6] A. Polman and P. Wiltzius, MRS Bull. **26**, 608 (2001).
  - [7] H. A. Macleod, *Thin-Film Optical Filters* (Hilger, London, 1969), Chap. 5.
  - [8] M. M. Sigalas, C. M. Soukoulis, C. T. Chan, and K. M. Ho, Phys. Rev. B **49**, 11080 (1994).
  - [9] V. Kuzmiak, A. A. Maradudin, and F. Pincemin, Phys. Rev. B **50**, 16835 (1994).
  - [10] M. M. Sigalas, C. T. Chan, K. M. Ho, and C. M. Soukoulis, Phys. Rev. B **52**, 11744 (1995).
  - [11] J. B. Pendry, A. J. Holden, W. J. Stewart, and I. Youngs, Phys. Rev. Lett. **76**, 4773 (1996).
  - [12] D. F. Sievenpiper, E. Yablonovitch, J. N. Winn, S. Fan, P. R. Villeneuve, and J. D. Joannopoulos, Phys. Rev. Lett. **80**, 2829 (1998).
  - [13] K. C. Huang, P. Bienstman, J. D. Joannopoulos, K. A. Nelson, and S. Fan, Phys. Rev. Lett. **90**, 196402 (2003); Phys. Rev. B **68**, 075209 (2003).
  - [14] W. Zhang, A. Hu, X. Lei, N. Xu, and N. Ming, Phys. Rev. B **54**, 10280 (1996).
  - [15] W. Zhang, A. Hu, and N. Ming, J. Phys. Condens. Matter **9**, 541 (1997).
  - [16] P. M. Bell, J. B. Pendry, L. M. Moreno, and A. J. Ward, Comput. Phys. Commun. **85**, 306 (1995).
  - [17] J. N. Winn, R. D. Meade, and J. D. Joannopoulos, J. Mod. Opt. **41**, 257 (1994).
  - [18] D. F. Edwards and R. H. White, in *Handbook of Optical Constants of Solids II*, edited by E. D. Palik (Academic, New York, 1991), p. 805.
  - [19] T. Chibuye, C. G. Ribbing, and E. Wäckelgård, Appl. Opt. **33**, 5975 (1994).
  - [20] Ph. Mavropoulos, N. Papanikolaou, and P. H. Dederichs, Phys. Rev. Lett. **85**, 1088 (2000).
  - [21] C.-G. Ribbing and A. Rung, Swedish patent 0104195-3 (2003).